Sedimentology (1993), **40**, 869–877

Entrainment of planktonic foraminifera: effect of bulk density

REINHARD OEHMIG

GEOMAR, Research Center for Marine Geosciences, Wischhofstraße 1–3, 2300 Kiel 14, Germany

ABSTRACT

Depositional hydrodynamics have been studied using settling rate distributions of Norwegian deep sea sediments (between Jan Mayen Island and the Vøring Plateau), together with Shields' critical shear stress velocities. Planktonic foraminifera are the dominant sand sized component of these sediments. The bulk density of the foraminifera was calculated from their settling velocity, sieve size and shape. Density decreases from 2·39 g cm^{-3} at 0·05 mm diameter to 1·37 g cm^{-3} at 0·35 mm diameter. These density and size data were used to construct a threshold sediment movement curve. From the similarity in their Shield's critical shear-stress velocities and the observed correlation of foraminifera size with decreasing percentage of fine fraction, it is concluded that the two components, the sand size foraminifera and the quartz and carbonate silt, are transport-equivalent.

INTRODUCTION

Hydrodynamics control the transport and accumulation rate of sediment, and the diversity and ecology of benthic communities. Sediment texture, because of its ability to record depositional hydrodynamics, can thus be used for palaeo-oceanographic interpretation. In this study, planktonic foraminifera are used to reconstruct depositional hydrodynamics, because they are both widespread and abundant, and their size distribution may reveal the threshold velocity for sediment movement (Altenbach *et al.*, 1988).

In order to determine the maximum post-depositional current velocity from the size distributions of foraminifera, the erosion velocity of the different sizes of foraminifera must be known. This velocity may be determined in three ways.

(1) Measurement in laboratory flumes as described by Southard *et al.* (1971), or measurement of the threshold velocities of individual tests placed on a fine sand substrate (synthetic sea floor) as conducted by Kontrovitz *et al.* (1979). The experimental technique of Southard *et al.* (1971) requires large quantities of abyssal sediment. The logistics in simulating a real sea floor, particularly its structural features, are extremely difficult and expensive.

(2) Determination *in situ* on the sea floor. So far this has only been done for shallow water (Young & Mann, 1985); deep sea experiments are difficult for logistical reasons, as stated under (1) above.

(3) Calculation of Shields' critical shear stress velocity from the Reynolds number; this velocity defines the beginning of sediment movement (Shields, 1936).

The original Shields' curve has been refined using selected experimental data (Miller *et al.*, 1977). Miller & Komar (1977) have applied this curve to a wide range of grain densities, and of fluid densities and viscosities. Grain density is an important parameter of Shields' relationship; however, since foraminifera tests are hollow and contain sea water, their *bulk* density must be used.

The purpose of the project reported here was to study the relationship between the bulk density and critical shear-stress velocities of the foraminifera. The textural characteristics of Recent sediments from the Norwegian Sea were analysed in order to obtain the depositional hydrodynamics. Shields' curve is valid for these sediments because *non-cohesive* calcareous coccoliths of medium and fine silt size form the bulk of the fine sediment (Lonsdale & Southard, 1974;

Huizhong & McCave, 1990; Samtleben & Schröder, 1990).

Surface sediments from the Norwegian Sea

Box core surface samples (0–1 cm) taken during a transect from the Vøring Plateau to Jan Mayen Island (Fig. 1) were prepared in order to determine the bulk density of the foraminifera tests (from Site 62) and the sediment textural characteristics from the complete transect of 17 surface samples. The transect is located along the Jan Mayen Fracture Zone (*Meteor* cruise 2/2; Gerlach *et al.*, 1986), passing the tops and flanks of various seamounts and submarine plateaus, and across the Vøring Plateau (Henrich *et al.*, 1989). Site 58 is located away from these submarine highs, in the abyssal environment of the Lofoten Basin (Fig. 1).

The sample from Site 62 (fraction >0·063 mm) was enriched in foraminifera by heavy liquid separation (Kachholz & Henrich, 1987), and sieved into restricted fractions. The average intermediate diameter (*b*-axis) of about 30 tests of each fraction was measured under a stereo-microscope (Table 1).

Two groups of samples were used for sedimentational analysis.

(1) Restricted sieve fractions (each about 0·15 g) of the foraminifera concentrate; the fractions were: <0·063, 0·063–0·09 mm, 0·09–0·1, 0·1–0·112, 0·112–0·125, 0·125–0·15, 0·15–0·2, 0·2–0·25 and >0·25 mm. Modal settling velocities of each fraction were used for calculating the bulk densities of foraminifera (Fok-Pun & Komar, 1983; Altenbach *et al.*, 1988).
(2) A complete fraction coarser than 0·063 mm (each about 1 g) of the 17 transect sediments.

After air was removed from the tests by exposing the immersed samples to a vacuum, both groups of samples were subject to sedimentational analysis.

Sedimentational analysis

The settling rate is more closely related to hydrodynamic sediment properties such as entrainability than it is grain size (Komar & Clemens, 1986), and therefore an advanced settling tube system, *MacroGranometer*™

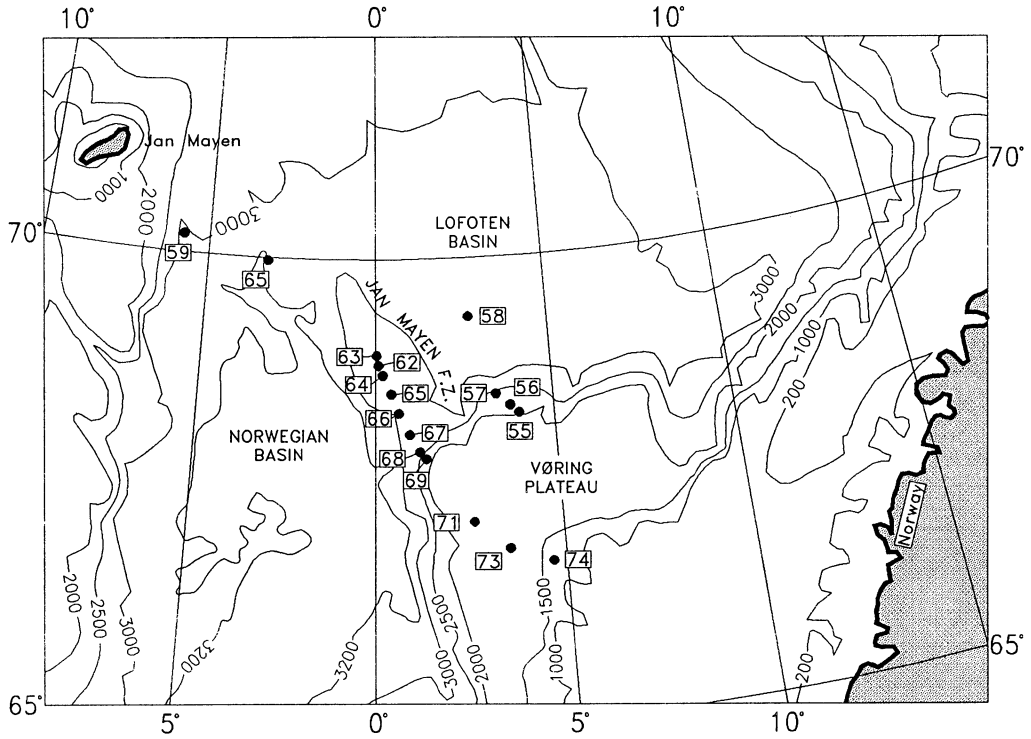

Fig. 1. Sample sites, located mostly on higher positions between the Lofoten Basin and the Norwegian Basin (after Perry *et al.*, 1980).

Table 1. Size fractions of planktonic foraminifera: data used for calculation of the bulk density.

d (mm)	v (cm s^{-1})	T (°C)	n (cm^2 s^{-1})	R_f (g cm^{-3})	Re	C_D	$R_{s\text{-Komar}}$ (g cm^{-3})	$R_{s\text{-Brezina}}$ (g cm^{-3})
0·053	0·22	23·04	0·00935	0·9976	0·13	181·58	2·262	2·388
0·086	0·35	23·07	0·00934	0·9975	0·32	76·00	1·823	1·885
0·115	0·52	23·11	0·00933	0·9974	0·64	40·87	1·730	1·768
0·121	0·57	22·13	0·00958	0·9977	0·72	35·84	1·731	1·787
0·138	0·61	20·94	0·00988	0·9979	0·85	32·97	1·676	1·671
0·166	0·72	20·86	0·00990	0·9980	1·21	21·98	1·522	1·567
0·228	0·93	22·35	0·00953	0·9976	2·23	12·58	1·369	1·398
0·280	1·47	22·09	0·00959	0·9977	4·29	8·77	1·514	1·467
0·351	1·72	22·31	0·00955	0·9976	6·32	6·21	1·397	1·368

d, average intermediate diameter (stereo-microscope); v, modal settling velocity (settling tube); T, arithmetic mean of the top and bottom temperatures in the sedimentation column; n, R_f, kinematic viscosity and density of fluid were calculated from T; Re, Reynolds' number was calculated from d, v and n; C_D, drag coefficient from the C_D–Re diagram for calculation of $R_{s\text{-Komar}}$; $R_{s\text{-Brezina}}$, bulk density as calculated with the C_D–Re–SF' equation of Brezina (1979).

(Brezina, 1979, 1980), was chosen in order to obtain settling rate distributions. This instrument uses a sensitive underwater balance which allows the resolution of even small differences (0·02 ψ) in the psi* settling rate distributions. The glass column of the *MacroGranometer* has an inner diameter of 20 cm and a sedimentation length of 192 cm. The water temperature is given in Table 1 for analyses of the group 1 samples. It was about 21°C for the group 2 samples.

In order to determine the settling velocity range over which the planktonic foraminifera are concentrated, the content of one typical polymodal settling velocity distribution of sediment coarse fraction was subdivided into preprogrammed psi settling velocity fractions (Oehmig, 1990). This was achieved by means of a *Sand Sedimentation Separator*™ (Brezina, 1989). The Sand Sedimentation Separator glass sedimentation column has the same dimensions as that of the *MacroGranometer*. At the bottom, two convergent conveyors transport the sediment into two alternating chambers. After the settling time of the first programmed psi settling rate has passed, the first chamber is replaced by a second one in which the second fraction accumulates; the first fraction is flushed out from the first chamber and dried on the porous bottom of a funnel. The second fraction accumulates in the second chamber until it is replaced by the first chamber, flushed out and dried on a second funnel. The third fraction continues accumulating in the first chamber, and so on.

* Psi (transcription of the Greek letter ψ) is a negative binary logarithm (=logarithm to the base 2) of a dimensionless settling rate. Middleton (1967) defined this unit to be analogous to phi (ϕ), the binary logarithm of a dimensionless grain size.

Bulk density of the foraminifera shells

The dominant foraminifera *Neogloboquadrina pachyderma* (Henrich *et al.*, 1989) has an approximately spherical shape. The shape, size and pertinent settling rate (v; Table 1) determine the bulk density of the foraminifera. This density was calculated from the drag coefficient, C_D, as a function of the Reynolds' number for sedimenting grains, Re:

$$C_D = \frac{40 \times (R_s - R_f)\, g\, d}{3 \times R_f\, v^2},$$

where R_s is the density of the solid (g cm^{-3}), R_f is the density of the fluid (g cm^{-3}), g is the acceleration due to gravity (cm s^{-2}) and d is the grain diameter (mm). Two methods for determining C_D were used.

(1) Using the data of Komar (1981, fig. 1), in which spherical grains are plotted on a C_D–Re (so called *Nikuradze*) diagram. Table 1 lists densities of the different foraminifera size fractions computed following the method of Fok-Pun & Komar (1983).
(2) Using the C_D–Re–SF' equation of Brezina (1979), where SF' is the hydrodynamic shape factor (for smooth spheres, $SF' = 1{\cdot}18$); his computer program is capable of producing any sedimentation variable such as the bulk density (Table 1) needed for this study.

The almost identical densities derived from using both methods (differences are due to reading errors from the *Nikuradze* diagram in Komar, 1981) decrease with increasing size of the planktonic foraminifera, as shown by Fok-Pun & Komar (1983) for *Orbulina universa*.

Critical shear stress velocity of foraminifera tests

The modified Shields' curve of dimensionless shear stress (θ_t) versus Reynolds number of transported grains (Re^*) has been presented by Miller *et al.* (1977, Fig. 2):

$$Re^* = \frac{10 \times d\, u^*}{n},$$

$$\theta_t = \frac{\tau_t}{(R_s - R_f)\, g\, d},$$

where u^* is the critical shear stress velocity (cm s^{-1}), n is the kinematic viscosity (cm^2 s^{-1}) and τ_t is the threshold shear stress ($= R_f u^{*2}$).

This curve was used to calculate the critical shear stress velocity u^* of the foraminifera from their diameter and bulk density, solving the equations above; $n = 0{\cdot}0183$ cm^2 s^{-1} and $R_f = 1{\cdot}0281$ g cm^{-3} for sea water at 0°C (Miller & Komar, 1977), and $g = 983$ cm s^{-2} at 68°N latitude in 2000 m of water. The resulting curves of u^* vesus d were plotted for each foraminifera density and for quartz density (2·65 g cm^{-3}; Fig. 3).

The critical shear stress velocity of the sand-sized foraminifera (the eight data points to the right) varies around 0·8 cm s^{-1} (stippled area in Fig. 3). Extension of this range of u^* to the quartz curve ($R_s = 2{\cdot}65$ g cm^{-3}) indicates that it is also valid for quartz and dense non-porous carbonate of medium silt size. The two data points showing exceptionally

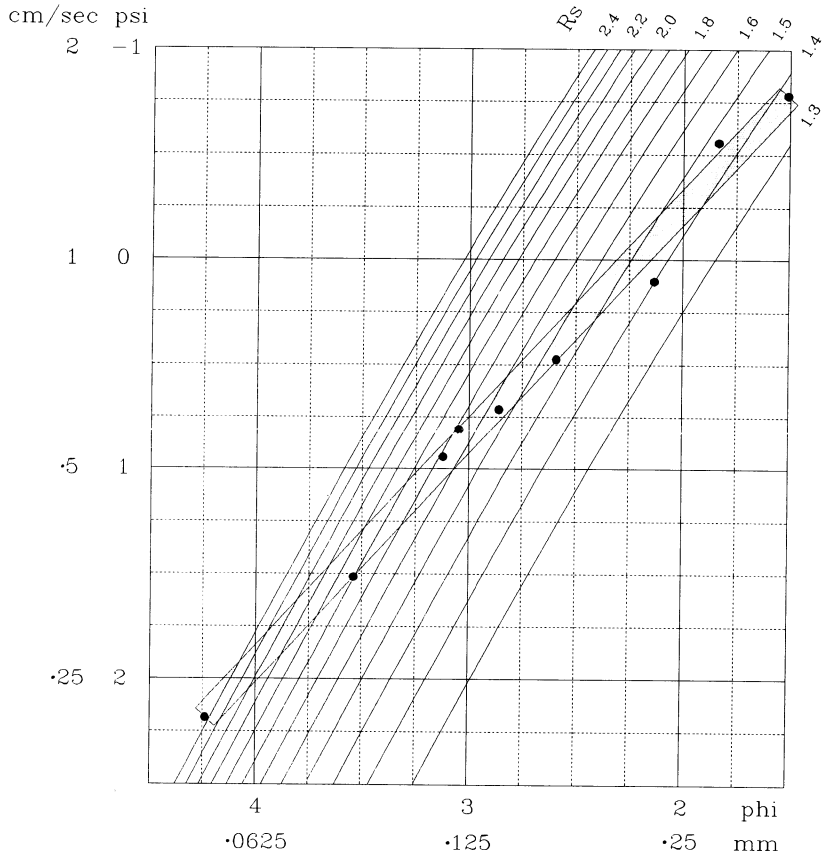

Fig. 2. Settling rate (psi) of foraminifera sieve fractions (phi) (closed circles). Lines of constant particle density (R_s) were plotted for $SF' = 1{\cdot}18$, distilled water at 22·2°C and $g = 981{\cdot}4$ cm s^{-2}, using the equation and program of Brezina (1979). Foraminiferal density decreases with grain size.

high values of u^* at average foraminifera diameters of 0·121 and 0·28 mm are due to the relatively high bulk densities of these size fractions (Table 1).

RESULTS

Texture

The sediment material comes from pelagic flux (mostly calcareous planktonic foraminifera and nannoplankton), ice-rafting, terrigeneous input and benthonic foraminifera (Henrich *et al.*, 1989). Figure 4 shows a typical polymodal settling velocity distribution of a Recent coarse sediment fraction. The following dominant components were identified in three settling rate fractions (Oehmig, 1990): mode 1, fast settling rate, large shells of agglutinated benthic foraminifera and *Pyrgo* sp.; mode 2, discoidal benthic foraminifera; mode 3, slower than $-1\,\psi$, typically -1 to $0\,\psi$, planktonic foraminifera.

The percentage of the fine fraction (<0·063 mm) is another important feature. Many components of this fraction are easily moved by common deep sea currents (Prell, 1977; Altenbach *et al.*, 1988; Huizhong & McCave, 1990); stronger currents probably reduce this percentage by winnowing (Hollister & McCave, 1984).

Both textural sediment parameters—the fine fraction percentage and the size of the planktonic foraminifera (mode 3)—are plotted in Fig. 5 in a sequence of decreasing fine fraction percentage. Sediments with a smaller amount of fine material contained larger planktonic foraminifera.

Foraminifera shells: indicators of bed load transport

The correlation of the size of the planktonic foraminifera mode with the fine fraction percentage (Fig. 5) can be explained by a hydrodynamic equivalence indicated by similar critical shear stress velocities of medium silt-sized quartz and sand-sized foraminifera (Fig. 3). However, the percentage of the medium silt is not known; instead, the percentage of the complete fine fraction <0·063 mm only has been determined. This could explain some scattering around a straight line relationship between the complete fine fraction percentage and the modal size of planktonic foraminifera.

Two major exceptions (arrows in Fig. 5) to the correlation can be explained by other influences.

(1) The sediment of Site 73 from the Vøring Plateau is strongly influenced by terrigeneous input. Considerable portions of quartz sand, silt and clay characterize this sediment (maximum 93% of the

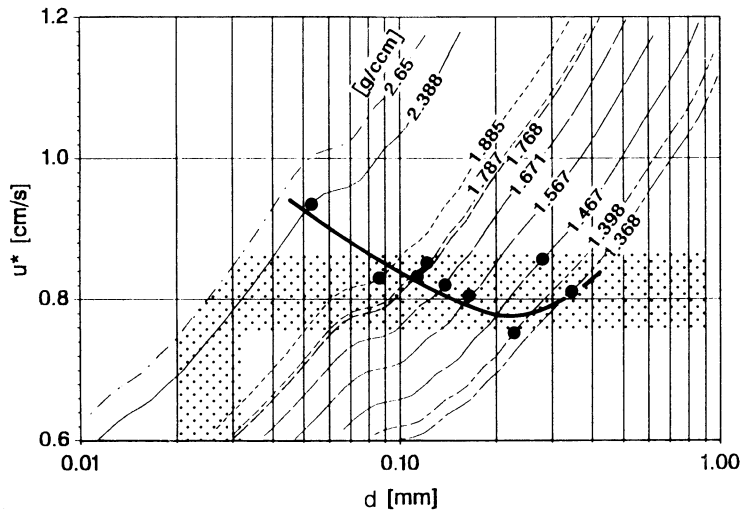

Fig. 3. Critical shear stress velocity u^* of planktonic foraminifera tests as a function of test diameter and bulk density (bold line, with a minimum u^* at 0·228 mm). The curves of u^* versus d were plotted for those bulk density values which were calculated from grain size and settling velocity of each foraminifera fraction (Table 1, columns 1, 2 and 9). The data points are the u^* values of the bulk density curve at the grain size of each foraminifera fraction. The stippled area is the range of silt (density 2·65 g cm^{-3}) equivalent in u^* values to the sand-sized foraminifera tests.

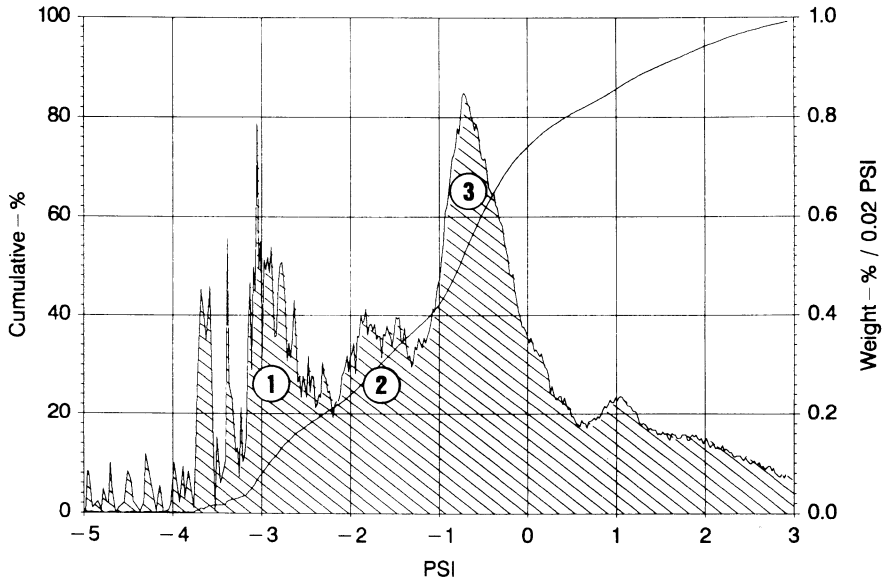

Fig. 4. A typical polymodal settling velocity distribution of surface sediments from the study area, Site 68. Mode 1 and 2: benthic foraminifera, mode 3: planktonic foraminifera, mainly *Neogloboquadrina pachyderma*.

<0·063 mm fraction). The quartz sand grains have a higher density and are smaller (less drag) compared with foraminifera of equivalent settling rate. Much faster bottom currents would be necessary to entrain these non-porous grains. Even with a shift to faster settling rates, a steeper flank of the main mode at the faster part of the psi settling rate distribution did not form (Fig. 5).

(2) The sediment at Site 58 from the abyssal plain of the Lofoten Basin is influenced by turbidity current deposits from the surrounding topographical highs (Eldholm & Windisch, 1974). A considerable portion of the slowly settling fine material of a turbidity current has probably been separated from the faster sinking sand-sized foraminifera and deposited elsewhere.

Grabert (1971, p. 1) studied foraminifera shells as tracers of sediment movement in a coastal lagoon. She found that 'the distribution of the sand grain sizes and of the foraminifera tests indicates that particles with the same hydraulic equivalent-diameter are not equivalent as to transport, because they are not found together. As to lateral transport, grains with the same sinking velocity are not transported together, but finer grain sizes are transport-equivalent to the foraminifera.' A similar relationship is commonly reported for the fast settling and easily entrainable large faecal pellets in contrast to the barely entrainable mud with low settling velocity (citations in Nowell *et al.*, 1981). However, before it can be stated that hollow foraminifera tests and massive silt grains found together in deep sea sediments were both transported as bedload, the depositional conditions must be viewed in detail.

Transport association versus lag deposit

Figure 6 shows two hypothetical size distributions of a foraminifera sand. A lag deposit forms a coarse distributional tail and a steep flank on the fine side, because of the winnowing of fine sediment below a certain grain size which is just entrainable. A transport association forms a fine tail. The steep flank on the coarse side represents the maximum grain size which can be just moved. The shape of the hypothetical curve on the left in Fig. 6 is similar to that in most of the distributions in Fig. 5, where the steep flanks on the left indicate that these foraminifera sands are transport associations (note that foraminifera size is increasing from the right to the left in the distributions in Fig. 5).

In all deposits in this study, the modal settling velocity of the planktonic foraminifera is faster than 0·11 $\psi = 0{\cdot}93$ cm s^{-1} (Fig. 5) and diameters are coarser than 0·228 mm (Table 1). Below this limit, tests are relatively rare and do not form a peak. Above this

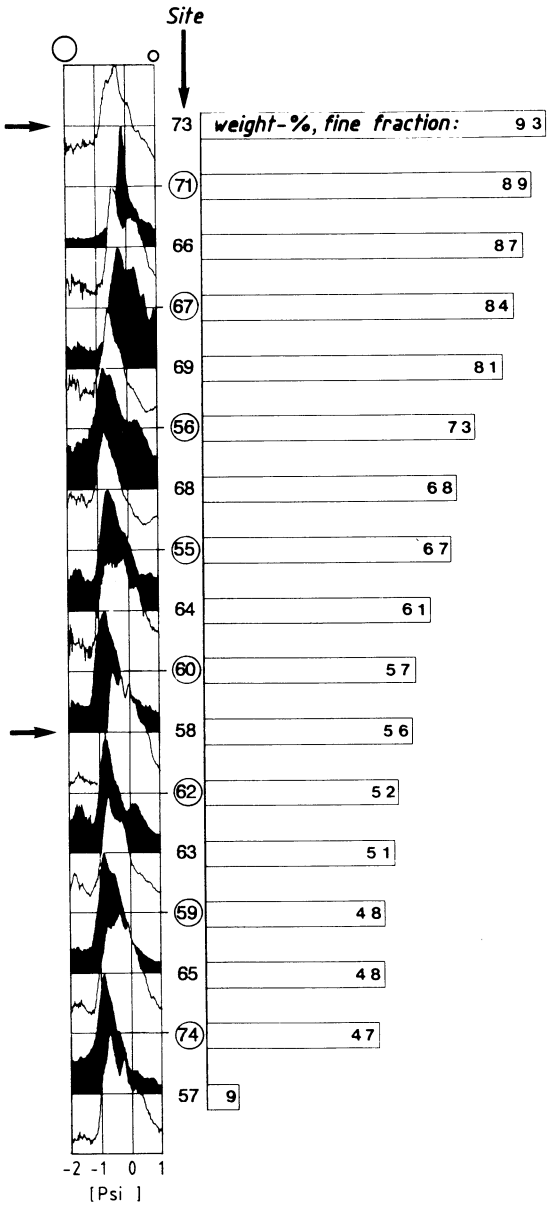

Fig. 5. Left: psi settling rate distributions display the dominant mode of the planktonic foraminifera, slightly shifting to higher velocities with decreasing percentage of the fine fraction (vertical axis is about 1‰/0·02 ψ). Right: the percentage of the fine fraction.

limit, the foraminifera are abundant, form a strong peak and their size is proportional to the critical shear stress velocity (Fig. 3). A lag origin of the latter foraminifera is improbable for two reasons.

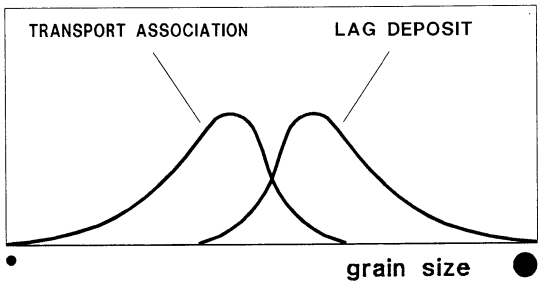

Fig. 6. Assumed shape of the size distribution expected for transport association and lag deposit.

(1) Larger tests are absent in low energy environments (Fig. 5, upper part).
(2) The fine part of the distribution is available as a tail: it was not winnowed (Fig. 5, lower part), as winnowing, the process of generating lag deposits, would remove the fine tail and form a steep flank.

Under the assumption that the critical shear stress velocity of the foraminifera is inversely proportional to their size, the lag formation is also improbable, because then the large tests would have to occur in low energy deposits and be less abundant in high energy deposits.

Hydrodynamic roughness of the sea floor

Recent sediments from the Norwegian Sea consist of a silty clay matrix and of a coarse fraction, mostly foraminifera (Henrich *et al.*, 1989). The observed correlation of larger foraminifera with lower percentage of the fine fraction (Fig. 5) can be explained by the effect of a hydrodynamic roughness of the sea floor. Larger foraminifera on the sea bottom or partly embedded in the fine sediment matrix create a floor roughness which increases turbulence and the entrainment of fine material. In contrast, smaller foraminifera are associated with the abundant fine fraction because of a low roughness and entrainment capability.

CONCLUSIONS

(1) There is an inverse relationship between size and bulk density of planktonic foraminifera (mainly *Neogloboquadrina pachyderma*); the bulk density, calculated from settling velocity, decreases with increasing diameter.
(2) Sand-sized foraminifera are transport-equivalent to quartz and carbonate silt due to the similar u^*.

The bulk density of the foraminifera and Shields' curve were used to calculate the critical shear stress velocity u^*; when plotted for different densities against size, u^* reaches a minimum at a diameter of 0·228 mm.

(3) The sediment was transported as bedload, for the following reasons: (i) the u^*-equivalence of the sand-sized foraminifera to the quartz and carbonate silt; (ii) surface sediments on elevated positions show a correlation of larger foraminifera with a lower percentage of the fine fraction; and (iii) the shape of the foraminifera settling rate distribution (steep flank on its faster part).

(4) Bottom hydrodynamic roughness and a selective reduction of the amount of slowly settling sediment have similar effects on sediment texture.

ACKNOWLEDGMENTS

The present study was conducted within the research project of the German Research Society (*DFG*) *Sonderforschungsbereich 313* at Kiel University. I thank J. Brezina (Neckargemünd, Germany), G. Unsöld, K. Lackschewitz and R. Henrich (all from Kiel) for discussions. M. Kontrovitz (Lawrenceville, New Jersey), C. J. Lovell (Oxon, England) and M. R. Talbot (Bergen, Norway) are thanked for their constructive review of the typescript. I gratefully acknowledge the assistance of S. Schultz and J. Schmeiss for settling analyses, R. Rössler and C. Scharfenberg for stereo-microscope measurements, J. Welling for review of the English and S. Körsgen for drafting. Of the two sedimentation instruments, designed and produced by J. Brezina, the *Sand Sedimentation Separator*™ was heavily subsidized by J. Brezina who also carefully edited the various drafts of the typescript.

REFERENCES

ALTENBACH, A.V., UNSÖLD, G. & WALGER, E. (1988) The hydrodynamic environment of Saccorhiza ramosa (BRADY). *Meyniana*, **40**, 119–132.

BREZINA, J. (1979) Particle size and settling rate distributions of sand-sized materials. In: *Partec—2nd Eur. Symp. on Particle Characterisation.*

BREZINA, J. (1980) Korngrößenanalyse sandkörniger Materialien. *Laborpraxis*, **4**, 18–26.

BREZINA, J. (1989) Sand Sedimentations-Analyse und Separation—mehr als 25 Jahre Forschung und Entwicklung. *Nachr, Dt. Geol. Gesell.*, **41**, 149–153.

ELDHOLM, O. & WINDISCH, C.C. (1974) Sediment distribution in the Norwegian–Greenland Sea. *Bull. geol. Soc. Am.*, **85**, 1661–1676.

FOK-PUN, L. & KOMAR, P.D. (1983) Settling velocities of planktonic foraminifera: density variations and shape effects. *J. Foram. Res.*, **13**, 60–68.

GERLACH, S.A., THIEDE, J., GRAF, G. & WERNER, F. (1986) *Forschungsschiff Meteor, Reise 2 vom 19. Juni bis 16. Juli 1986.* Berichte Sonderforschungsbereich 313, Universität Kiel.

GRABERT, B. (1971) Zur Eignung von Foraminiferen als Indikatoren für Sandwanderung. *Dt. Hydrogr. Z.*, **24**, 1–14.

HENRICH, R., KASSENS, H., VOGELSANG, E. & THIEDE, J. (1989) Sedimentary facies of glacial–interglacial cycles in the Norwegian Sea during the last 350 ka. *Mar. Geol.*, **86**, 283–319.

HOLLISTER, C.D. & MCCAVE, J.N. (1984) Sedimentation under deep-sea storms. *Nature*, **309**, 220–225.

HUIZHONG, W. & MCCAVE, J.N. (1990) Distinguishing climatic and current effects in mid-Pleistocene sediments of Hatton and Gardar Drifts, NE Atlantic. *J. geol. Soc.*, **147**, 373–383.

KACHHOLZ, K.D. & HENRICH, R. (1987) *Verschiedene Experimente mit der Sedimentationswaage.* Berichte Sonderforschungsbereich 313, Universität Kiel.

KOMAR, P.D. (1981) The applicability of the Gibbs equation for grain settling velocities to conditions other than quartz grains in water. *J. sedim. Petrol.*, **51**, 1125–1132.

KOMAR, P.D. & CLEMENS, K.E. (1986) The relationship between a grain's settling velocity and threshold of motion under unidirectional currents. *J. sedim. Petrol.*, **56**, 258–266.

KONTROVITZ, M., KILMARTIN, K.C. & SNYDER, S.W. (1979) Threshold velocities of tests of planktic foraminifera. *J. Foram. Res.*, **9**, 228–232.

LONSDALE, P. & SOUTHARD, J.B. (1974) Experimental erosion of North Pacific red clay. *Mar. Geol.*, **17**, M25–M34.

MIDDLETON, G.V. (1967) Experiments on density and turbidity currents. 3. The deposition of sediment. *Can. J. Earth Sci.*, **4**, 475–505.

MILLER, M.C. & KOMAR, P.D. (1977) The development of sediment threshold curves for unusual environments (Mars) and for inadequately studied materials (foram sands). *Sedimentology*, **24**, 709–721.

MILLER, M.C., MCCAVE, J.N. & KOMAR, P.D. (1977) Threshold of sediment motion under unidirectional currents. *Sedimentology*, **24**, 507–527.

NOWELL, A.R.M., JUMARS, P.A. & ECKMAN, J.E. (1981) Effects of biological activity on the entrainment of marine sediments. *Mar. Geol.*, **42**, 133–153.

OEHMIG, R. (1990) Die Isolierung von Sinkgeschwindigkeitsfraktionen mit dem Sand-Sedimentation-Separator (3S)™. In: *Sedimentation im Europäischen Nordmeer: Abbildung und Geschichte der ozeanischen Zirkulation* (Ed. by J. Thiede, S. Gerlach & R. Oehmig), pp. 251–286. Berichte Sonderforschungsbereich 313, Universität Kiel.

PERRY, R.K., FLEMING, H.S., CHERKIS, N.Z., FEDEN, R.H. & VOGT, P.R. (1980) *Bathymetry of the Norwegian–Greenland and Western Barents Seas. Geol. Soc. Amer. Chart*, **MC-21**. Naval Research Laboratory, Washington, D.C.

PRELL, W.L. (1977) Winnowing of recent and quaternary deep-sea sediments: Colombia Basin, Caribbean Sea. *J. sedim. Petrol.*, **47**, 1583–1592.

SAMTLEBEN, C. & SCHRÖDER, A. (1990) *Coccolithophoriden-Gemeinschaften und Coccolithen-Sedimentation im Europäischen Nordmeer—Zur Abbildung von Planktonzönosen im Sediment*. Berichte Sonderforschungsbereich 313, Universität Kiel.

SHIELDS, A. (1936) Anwendung der Ähnlichkeitsmechanik und der Turbulenzforschung auf die Geschiebebewegung. *Mitteilungen Preussische Versuchsanstalt für Wasserbau und Schiffbau*, **26**, 1–42.

SOUTHARD, J.B., YOUNG, R.A. & HOLLISTER, C.A. (1971) Experimental erosion of calcareous ooze. *J. Geophys. Res.*, **76**, 5903–5909.

YOUNG, R.A. & MANN, R. (1985) Erosion velocities of skeletal carbonate sands, St Thomas, Virgin Islands. *Mar. Geol.*, **69**, 171–185.

(Manuscript received 25 February 1992; revision accepted 17 March 1993)